

Bottom-layer solutions for 60 GHz millimeter-wave wireless networks: modulation and multiplexing access techniques

Claudio Estevez¹ · Cesar Azurdia¹

Published online: 1 April 2015

© The Author(s) 2015. This article is published with open access at Springerlink.com

Abstract Wireless technologies are an essential communication means that transform a branched localized fixed meshwork into a ubiquitous disconnected network. A clear trend shows that cells are becoming smaller, homogeneously distributed, operating at higher carrier frequencies, and more energy conscious. This points toward wireless picocell systems that implement millimeter-wave (mm-wave) modulation. In this work various techniques are proposed, which are oriented to specific traits of the 60-GHz mm-wave band. Two techniques oriented to solve physical and data-link layer issues are proposed. Single carrier frequency division multiple access (SC-FDMA) is proposed as the technology to be implemented at the physical layer, and a variable slot time multiplexing access technique, called variable slot time-time division multiple access (VST-TDMA), with a conscious energy-conservation protocol, is proposed for the data-link (MAC) layer. SC-FDMA with pulse shaping is implemented to minimize the peak-to-average power ratio of the system, which reduces energy consumption. The multiplexing access technique takes advantage of the reduced cell size by multiplexing data in the time domain, this allows the reduced number of users to utilize the entire available bandwidth. Incorporated into the access protocol is the option of energy pacing or even self-sustainability if an energy harvesting device is present. Self-sustainability can be achieved at the cost off throughput, some techniques are discussed to relieve this trade-off condition. Also, a thorough discussion is included on battery energy depletion, even with an energy harvesting device present, to further increase the through-

put performance. Since using SC-FDMA reduces the energy consumption, it enables VST-TDMA to operate at higher speeds under self-sustainability mode. Overall the proposed set of solutions showed independently significant improvements to the system. It is also discussed how these techniques coalesce conveniently by working in unison, improving the energy efficiency and throughput capabilities of 60-GHz systems.

Keywords 60 GHz · Energy self-sustainability · Millimeter-wave · Peak-to-average power ratio (PAPR) · Single carrier frequency division multiple access (SC-FDMA) · Variable slot time-time division multiple access (VST-TDMA)

1 Introduction

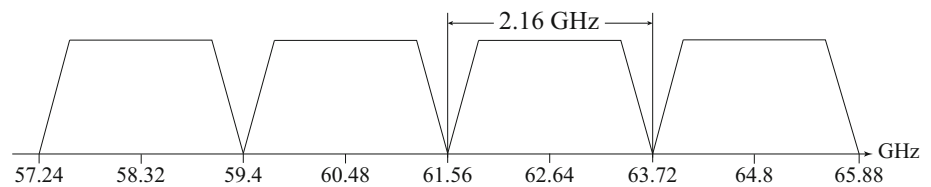
Historical trends portray that wireless technology is evolving, reaching maturity at the frequencies below 5 GHz and pushing for real estate in the higher portion of the spectrum. For example: One of the current most ubiquitous Wireless Local Area Network (WLAN) technologies is Wireless Fidelity (WiFi), which using a 2.4/5 GHz modulating frequency, channel widths of 20/40 MHz, multiple-input multiple-output (MIMO) antenna arrays, orthogonal frequency division multiplexing (OFDM), and dense quadrature amplitude modulation (QAM) constellations can reach a maximum of 600 Mbps [9,31], indicating that this technology is reaching its mature stages and it will become increasingly difficult to make significant improvements over relatively short time periods. For this reason mm-wave technology is becoming the new alternative for Wireless Personal Area Networks (WPAN) [35,54,59]. Due to their limited size these access points are sometimes referred to as picocells

✉ Claudio Estevez
cestevez@ing.uchile.cl

Cesar Azurdia
cazurdia@ing.uchile.cl

¹ Avenida Tupper 2007 Of. 503, Santiago, Chile

Fig. 1 ECMA-387 operating frequency range and band allocation



[33,36,49] or (less frequently) microcells [22]. mm-Wave systems have already proven to transmit at 2.5 Gbps [14], using simple techniques. To achieve these high bitrates it is beneficial to have large bandwidths, and make efficient use of this resource. The 60-GHz frequency band is attractive to throughput-demanding applications, such as: WPANs [50,53] and e-Health [21]. It is also a good candidate for access network services convergence.

While spectrum has become scarce at microwave frequencies, it is plentiful in the mm-wave domain. Cellular systems, which are in the microwave spectrum region, are characterized by having extremely precious but limited spectrum. Several initiatives and proposal are ongoing to expand the current cellular bandwidth within the microwave frequency range [11], which is not enough to achieve the capacities needed by 5G systems and the devices connected to the Internet of Things (IoT). There is a vast amount of spectrum available at the mm-wave frequency bands, ranging from 3 to 300 GHz [11,17,44,46,58]; therefore, mm-wave frequency bands are being proposed to be used in 5G cellular networks.

It is difficult to prognosticate what 5G networks will look like and what components will it incorporate. 60-GHz technology is a strong contender for 5G short-range access networks. A time-multiplexing protocol is an appealing solution because of the small cell size, frequency reuse, and reduced number of users per cell, all which point toward the effective and flexible use of the bandwidth. Additionally, the uncertainty of what components will 5G network be composed of, requires the design of a versatile MAC protocol. For example: A protocol that can perform quality of service (QoS) in both upstream and downstream, reserve time for processes other than multiplexing data, and the ability to dynamically adjust the energy consumption, and the capability to shift the bandwidth to where it is needed (upstream/downstream/symmetric) is a good candidate for WLAN/WPAN. If we add the available bandwidth found in the 60 GHz region, this protocol is an excellent candidate for 5G networks (more on these topics in Sect. 3.2).

Initial attempts to standardize the 60 GHz frequency range already exists. Among these initiatives are the ECMA-387 standard [26], 802.11ad-2012 [61], and the IEEE 802.16 standard [24,25]. One particular interest to our work is the band allocation of ECMA-387. It divides the operating frequency range (57.24 65.88 GHz) in four bands, as shown in Fig. 1. Several motives for having a low number of bands exist, such

as: less expensive (simpler filter design) and low number of users per picocell. Since there are low number of users per cell, it is not necessary to divide the usable spectrum into many bands, it is more efficient to assign ample bandwidth to each user (due to the small cell size), having in mind that there could potentially be a single user, than to reserve a reduced portion to the band leaving other frequencies unused. Therefore, frequency multiplexing is not an efficient approach in small cells, for this reason the focus of this work is to design a time-domain multiplexing technique with efficient time-allocating capabilities.

In this work a time multiplexing technique, denoted here as variable slot time-time division multiplexing access (VST-TDMA), is proposed. It has a self-adjusting time slot algorithm with a cyclic process that reserves time slots as they are requested. The requests are performed in a preemptive manner, such that when the slot assignment is performed, the base station is utilizing information that was obtained ahead of time. This is the reason the base station can allocate the exact amount of time necessary without having to estimate or guess. The serviced node (SN) does not need to adjust to a predetermined slot time, as with most types of time-based multiplexing techniques. Even though VST-TDMA is referred as a TDMA-based protocol it differs significantly from the standard mechanisms. The versatility of VST-TDMA expands the fix-time reservation of TDMA to a flexible and dynamic-time reservation ideology. VST-TDMA is not limited to data reservation, it also allows an easy incorporation of any process that needs to reserve channel access. Various useful processes could be implemented without modifying the algorithm, a few examples are: idle time and QoS. In wireless access networks energetically self-sustainable nodes are desirable due to the additional mobility it can provide by reducing (or eliminating) charging times. A node with a low energy reserve that is equipped with an energy-harvesting device can insert an idle-time process into the frame transmission cycle to allow the device to recharge, by trading-off throughput, as suggested in [27,28]. Another advantage of VST-TDMA is that QoS can be easily implemented, for example, if a node has time-sensitive information, the algorithm can switch to smaller and more frequent process reservations such that the effective throughput remains the same but the stream's overall delay is reduced. Also, different priority level traffic can have different reservation frequency privileges and different reser-

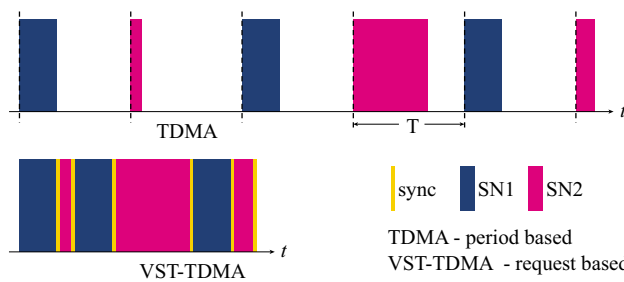


Fig. 2 Comparison between time allocation schemes VST-TDMA versus TDMA

vation time frame duration. A graphical comparison between time division multiple access (TDMA) and VST-TDMA is portrayed in Fig. 2.

The proposed multiplexing technique can be implemented in many types of networks. Its design is aimed to improve the performance of networks that have essentially two traits: (1) small cell, and (2) throughput demanding. Small cells imply few users per cell and therefore it is difficult to justify the use of frequency division multiplexing techniques. An efficient time-based multiplexing technique allows the bandwidth to be fully utilized. 60-GHz mm-wave technology fulfills well this role and for its high throughput capabilities it is the main motivator for designing VST-TDMA.

2 Background

Important content is included in this section to provide relevant information regarding modulation topics and related work in the MAC protocol field. This will help to better understand some modulation concepts discussed in this work and to emphasize some differences between VST-TDMA and other multiple access techniques.

2.1 Physical layer design

The IEEE 802.16 standard specifies four different physical layer (PHYs) solutions, including two single-carrier (SC and SCa) modes, OFDM, and a mode based on orthogonal frequency division multiple access (OFDMA) (IEEE 2004a) [24, 25]. For further details regarding the four PHYs solutions within the IEEE 802.16 standard, we suggest the readers to focus in [57] and [19]. One single carrier (SC) mode, which has been specified for frequency bands between 10 and 66 GHz, targets non-directed line-of-sight (LOS) communication links, whereas all other modes are designed for frequency bands below 11 GHz that must cover Non-LOS (NLOS) links [24, 25]. The initial version of the standard (IEEE 802.16-2001) specified only single-carrier PHY [24]. It targets frequency bands between 10 and 66 GHz, in which

non-directed LOS communication is mandatory due to the propagation characteristics [57]. Under non-directed LOS conditions the effects of multipath propagation, the delay spread of the system, is significantly reduced.

New wireless communication standards, such as the 3rd Generation Partnership Project (3GPP) long-term evolution (LTE), employ OFDM-based techniques for spectral efficiency. Despite the benefits offered by the newly introduced standards, the power amplifier of the mobile terminal has to accommodate higher peak-to-average power ratios (PAPR) than prior standards, such as wideband code division multiple access (WCDMA), code division multiple access (CDMA), and enhanced data rates for GSM evolution EDGE [15]. As a result, PAPR plays an important role in the design of wireless communication systems because power amplifiers are usually operated in the linear mode rather than the saturation mode. A bandlimited signal with high PAPR requires a large back-off to guarantee that the power amplifier operates inside its linear region in order not to distort the transmitted signals [7, 38, 39]. In addition, signals with high PAPR require higher dynamic ranges of digital-to-analog converters (DAC) at the power amplifier. In the 3GPP LTE standard, the technologies being implemented consist of single carrier frequency division multiple access (SC-FDMA), as well as OFDMA. Both of these technologies are based on OFDM techniques; however, SC-FDMA is being recommended as the uplink access technology due to its lower PAPR [7, 9, 38, 39]. To comply with the initial version of the IEEE 802.16-2001 standard, which species the use of a single carrier system for frequency bands between 10 and 66 GHz, we propose the implementation of SC-FDMA as the transmission scheme to be implemented by the SNs for uplink and downlink. Further, a system with a low PAPR is beneficial to the SNs, which are battery operated devices, because of the potential power savings. In the next sub-section we will describe in more details the SC-FDMA system, as well as the signals produced in the system.

2.1.1 Overview of the SC-FDMA system

SC-FDMA is also known as a discrete Fourier transform (DFT) spread OFDMA scheme because time domain symbols are transformed to the frequency domain via the DFT before OFDMA modulation. The orthogonality is due to the fact that each user occupies different orthogonal subcarriers in the frequency domain [38, 39]. The transmitter in a SC-FDMA system converts a binary input signal into a sequence of modulated subcarriers. In Fig. 3 we find a graphical description of how the transmitted SC-FDMA symbols are generated, as well as the nomenclature used throughout the rest of this manuscript, in the time and frequency domain. At the input of the transmitter, a baseband modulator transforms the binary sequence to a multilevel

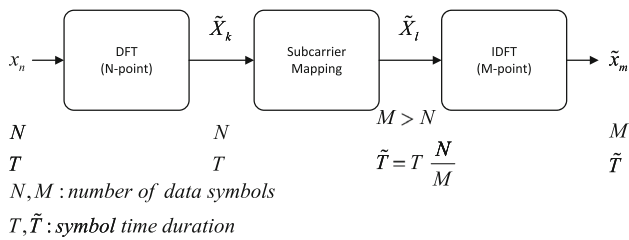


Fig. 3 Block diagram of the SC-FDMA symbols expressed in the time and frequency domain

sequence of complex numbers using one of several digital modulation techniques. The transmitter groups the modulated symbols, $\{x_n\}$, into blocks each containing N symbols, $\{x_n : n = 0, 1, 2, 3, \dots, N - 1\}$. The first step in modulating the SC-FDMA subcarriers is to perform an N -point DFT to generate a frequency domain representation of the input symbols. The frequency domain samples after DFT are expressed as $\{\tilde{X}_k : k = 0, 1, 2, 3, \dots, N - 1\}$. Subcarrier mapping is then performed, and each of the DFT outputs is mapped to one of the transmittable M ($> N$) orthogonal subcarriers. We have that $Q = \frac{N}{M}$, where Q is the bandwidth expansion of the symbol sequence, also known as the spreading factor. The frequency domain samples after subcarrier mapping are denoted as $\{\tilde{X}_l : l = 0, 1, 2, 3, \dots, M - 1\}$.

In SC-FDMA, subcarrier mapping can be achieved using one of several existing methods. The most common methods are the localized and distributed subcarrier modes [7, 9, 38, 39]. In the distributed subcarrier mode, the DFT outputs are spread over the entire bandwidth and zeros are introduced in the unused subcarriers. A special case of distributed SC-FDMA is known as interleaved SC-FDMA. Whereas in the localized subcarrier mapping mode, the outputs of the DFT are occupied by consecutive subcarriers, and the rest of the unused subcarriers are filled with zeros. The interleaved mode of SC-FDMA is more desirable than the localized mode in terms of PAPR and power efficiency [37, 39]. After the subcarrier mapping, an M -point inverse DFT (IDFT) transforms the amplitudes of the subcarriers into a complex time-domain signal. Each complex time-domain signal is modulated into a single frequency carrier, and the symbols are transmitted sequentially. After an M -point IDFT is applied, and the complex time-domain symbols are denoted as $\{\tilde{x}_m : m = 0, 1, 2, 3, \dots, M - 1\}$.

The transmitter performs two other signal processing operations previous to transmission. The output of the IDFT is followed by a cyclic prefix (CP). The CP is inserted to prevent intersymbol interference (ISI), which is due to multipath propagation. Certain subcarriers are used to insert a set of symbols to accommodate the cyclic prefix. The cyclic prefix is a copy of the last fraction of the most recent block, which is added to the beginning of the next block. The CP is very important for two reasons: it acts as a guard time

between consecutive blocks, and since the CP is a copy of the last part of the previous block, the system is converted into a discrete time circular convolution between the transmitted data block and the channel impulse response [39]. The complex time-domain passband signal to be transmitted for a block of data is given as follows

$$x(t) = e^{jw_c t} \sum_{m=0}^{M-1} \tilde{x}_m p(t - m\tilde{T}), \quad (1)$$

where $p(t)$ is the baseband pulse implemented, and w_c is the frequency of the passband carrier implemented in the system. The baseband pulse is implemented to bandlimit the transmitted signal and reduce the out-of-band signal energy [23, 39]. In our work we implement the traditional root raised cosine (RRC) pulse because it is the one proposed by the 3GPP standard in the transmitter and receiver of the user equipment (UE) and base station (BS) [1, 2].

The time-domain symbols of the localized and interleaved SC-FDMA systems were initially derived by Myng et al. [38]; therefore, for a complete derivation of the time-domain signals we suggest the readers to refer to [38]. In general, the time-domain signals produced by the localized SC-FDMA (SC-LFDMA) system are exact copies of the input symbols. These exact copies are found in the N -multiple sample positions, whereas the in-between values are a summation of all of the input symbols from a given input block. These in-between values are the ones that end up increasing the PAPR of the SC-LFDMA system. Whereas for the interleaved SC-FDMA (SC-IFDMA) system, the resulting time-domain symbols are simply a repetition of the original input symbols.

2.2 Work related to time-based access schemes

Most cellular technologies rely on time-based multiplexing techniques, mainly time division multiple access (TDMA). Some examples of these are GSM [56], D-AMPS [5], PDC, iDEN, PHS, IEEE 802.16a (WiMax) [60], Bluetooth [52], TD-SCDMA, ITU-T G.hn, LTE, Advanced LTE (A-LTE), and many others. Not all these examples are exclusively TDMA-based, some like LTE and A-LTE also have frequency multiplexing techniques. The basic operation of TDMA is to split the time domain in equal length time slots. Each slot is assigned to a user for the entire duration of the slot. In the case of TDD, time division is used to provide a half-duplex link, this is done by using the allocated time for either upstream or downstream transmissions.

There has been much work in TDMA-based protocols. Some are briefly discussed here, in particular those that share similar attributes with VST-TDMA. The protocols discussed are: client-weighted medium-transparent MAC

protocol (CW-MT-MAC) [29], process-stacking multiplexing access (PSMA) [20], Dynamic TDMA Scheduling (D-TDMA Scheduling or DTS) [13], packet reservation multiple access/dynamic allocation (PRMA/DA) [32], resource auction multiple access (RAMA) [4], slot reservation demand assignment multiple access (SRDAMA) [34], quality of service collision-free Receiver-Oriented MAC (QoS-CROMA) [18], and time division multiple access/frequency division duplexing (TDMA/FDD) [6], sensor-MAC (S-MAC) [63], timeout-MAC (T-MAC) [55], pattern-MAC (P-MAC) [65], Medium Reservation Preamble based MAC (MRPM) [51], adjustable sleep-mode MAC (AS-MAC) [64], Aloha [3], and Slotted Aloha [45]. CW-MT-MAC is a cross-layer (physical-data link) MAC protocol designed specifically for 60-GHz cells. It not only manages the flow of data through the wireless cell, but it also allocates the wavelength resources to each cell. Resources are allocated by demand, clients with higher demand are assigned greater priorities. The demand is determined by the number of active users per cell, where active users are those that consistently request resources. PSMA is the predecessor of VST-TDMA, so it shares many similarities, including the preemptive scheduling and the energy efficiency. The main difference is that PSMA is oriented to sensor networks as previous work only discusses unidirectional (upstream) transmissions. Another important difference is that in VST-TDMA, alternative energy profiles are proposed such that the throughput is a function of the available charge and not necessary fixed at the energy self-sustainable transmission rate (which decrease significantly the bit rate). D-TDMA is very similar to TDMA, with the exception that the time slots are dynamically assigned and several time slots in a row can be assigned to a single user if the system determines this is the optimal choice. In PRMA/DA each node can request a specific number of slots, the information is sent through the frame header. Time slot assignment is cyclic and can be reserved. Slots are assigned in the same manner than slotted ALOHA. In RAMA time slots are auctioned. There is a contention period where nodes “bid”, the base station determines which node has the highest priority and based on this criteria it assigns time slots. SRDAMA shares some similarities with VST-TDMA in the sense that it has a request-allocate mechanism, nevertheless in SRDAMA this is not done in a preemptive manner and it is based on Slotted ALOHA, which means slot times are fixed. In QoS-CROMA the base station can be programmed to service the surrounding nodes based on any priority criteria. The technique relies on an isotropic architecture as the base station is sending information to one node, while possibly sending an acknowledgement signal (within the same frame) to another node. Each node is programmed to ignore the part of the information that does not belong to it. This reduces latency and improves the effective throughput. TDMA/FDD uses frequency division duplexing, as the name suggests, to

multiplex the downstream and upstream data using different frequency bands. This avoids collisions between these types of data. It also has control time slots interleaved (much less frequent) with the data time slots. These slots provide service requirements information regarding the data slots, and enables the capability to provide QoS. S-MAC, T-MAC, P-MAC, and AS-MAC are all from the same family and variants of S-MAC. S-MAC is a MAC protocol that has an active/sleep state duty cycle, where reducing the duty cycle saves more energy (it sleeps for a longer periods of time). The duty cycle can be adjusted based on the application’s throughput and energy requirements. T-MAC, P-MAC, and MRPM have a few improvements over S-MAC but the basic operation is the same and they all have in common that the frame size has a fixed length. AS-MAC works slightly differently, it works in a similar way than S-MAC and T-MAC, but it has a variable sleep time. This allows and extra variable for optimization, but creates a more complex system as this scheme expects neighboring nodes to synchronize sleep times. AS-MAC shares a similar scheme than VST-TDMA in the sense that energy consumption can be controlled by the sleep time. Nevertheless none of the protocols from the S-MAC family have a preemptive system to compute the necessary active time. It should be mentioned that some of the MAC protocols discussed here are oriented for wireless sensor networks, but what is interesting to this work is the multiplexing techniques used, the energy efficiency, and other strengths and weaknesses that stand out. In all these cases, with the exception of AS-MAC, time slots or frames are of fixed length, this simplifies synchronization, though there are techniques that allow to further compress the time slots, so that there is no time wasted and synchronization is maintained. An example of this is the techniques used to synchronize and reserve resources in VST-TDMA, described in Sect. 3.2. Aloha and Slotted Aloha are contention-based protocols, rather than reservation-based. These are well-known protocols and can serve as a good mean for comparison.

3 Proposed bottom-layer solutions

In this section we will give a brief description of the proposed bottom-layer solutions for the 60 GHz mm-wave wireless communication systems. For the PHY, SC-FDMA is proposed as the transmission scheme. In the access control layer (within the data-link layer) resides VST-TDMA, which is a protocol that performs multiplexing in the time-domain by varying the user slot time, hence the name. This protocol is able to achieve energy self-sustainability given that it is equipped with an energy harvesting device. The details of how a variable time slot is achieved and energy self-sustainability is implemented are in Sect. 3.2.

3.1 Physical layer considerations

To fulfill with the initial requirements of the IEEE 802.16-2001 standard, which specifies the use of a single carrier system for frequency bands between 10 and 66 GHz, we propose the implementation of the SC-FDMA technology as the transmission scheme to be implemented in the uplink and downlink. SC-FDMA is characterized as being an energy efficient system because of its low PAPR compared to that of the OFDM scheme. A system with a low PAPR is beneficial to the SNs implemented in our network topology, which are battery operated devices, because of power limitations. The SC-FDMA system will be analyzed in terms of PAPR for the interleaved and localized subcarrier mapping modes and different modulation schemes. The performance of the proposed system will be compared with the OFDM scheme in terms of PAPR efficiency. The OFDM scheme has been proposed by several researchers as the technology to be implemented for the 60 and 70 GHz-bands [47,48,62], as well as by the IEEE 802.16 [24,25] and ECMA-387 [26] standards. Further, OFDM-based systems are being studied and proposed as one of the technologies to be implemented at the physical layer of 5G systems [12,17,44,46,58]. For example, OFDM-based systems combined with MIMO techniques are being suggested as the key technologies to be used at the physical layer of 5G cellular networks.

3.2 Variable slot time TDMA

VST-TDMA, like TDMA, performs multiplexing access in the time domain. VST-TDMA schedules processes and the process time is reserved when requested and for the time requested, i.e., there is a variable slot time duration. A process can be the transmission of data, transmission of control signals, or just the insertion of idle time (for energy conservation purposes). It is oriented to work in the 60 GHz mm-wave spectrum region for several reasons. As mentioned earlier this region of the spectrum exhibits high atmospheric absorption due to the resonance with the oxygen molecules. This causes a drastic cell size reduction compared to neighboring carrier frequencies. This limits considerably the amount of end-systems found in the cell. For this reason a multiplexing technique that does not divide the frequency band into sub-bands is an attractive option. Dividing into sub-bands means less bandwidth per band. In a scenario where there are less devices in the cell than sub-bands will leave unused spectrum and therefore will be a wasteful strategy. It is more efficient to multiplex in the time domain as devices request access. This motivates the use of a TDMA-based protocol. Another reason for using a high-bandwidth single-channel strategy is frequency reuse. The 60-GHz carrier frequency is usually modeled as a NLOS wave. This technology is expected to have an effective coverage radius in the range of 1–10 meters,

depending mainly on the beamwidth of the antenna and gains used. In these scenarios frequency reuse is a viable option that should be exploited, therefore having a single-channel time-based multiplexing technique is an ideal solution. Another consideration adopted in the design of VST-TDMA is related to the high directionality of the antennas. Narrow beamwidth transmissions exacerbate the hidden-node and exposed-node problems because neighbor discovery is more difficult to achieve with non-isotropic waves. This discards the use of any carrier-sense multiplexing access (CSMA) technique. In VST-TDMA, the only requirement for successful multiplexing is that all the nodes have the base station in their field of view and vice versa, but it is not necessary that the nodes sense each other. Hence, VST-TDMA is not affected by either of these problems.

The subsections that follow explain some of the most important features of VST-TDMA, these are: the global time pointer, packet encapsulation, communication dynamics, and energy self-sustainability scheme.

3.2.1 Global time pointer

To organize the transmissions a global time pointer is set by the base station, also referred as the Wireless Access Point (WAP). In the event that an internal WAP process or a node requests the reservation of the channel, this process is scheduled at the time stored in the global time pointer and the pointer is shifted by the amount of time requested, in practice a buffer time is also inserted for processes that require the use of the channel to account for wave propagation time. If the current time reaches the global pointer time it means there are no pending tasks and the WAP switches to listen mode. All nodes operate at the same frequency in both upstream and downstream directions, to multiplex this bidirectional scheme TDD is used.

3.2.2 Packet encapsulation

Before explaining the packet encapsulator, the neighboring processors will be discussed. The packet encapsulator processor is surrounded by the queue and main processors. The queue has a very simple task, it gathers high level packets and releases them when the main processor requests them (when it is ready to send). Once requested the queue releases all the packets (there could be a specified maximum) in its buffer. The packet encapsulator, which will be discussed in more detail below, gathers all the queue packets and encapsulates these in a frame. Once encapsulated the frame is transferred to the main processor, which stores the destination address (among other information) in the header and sends out the frame. The packet encapsulator has a crucial role in the VST-TDMA scheme, so it will be discussed in more detail. The encapsulator, as expected, gathers the net-

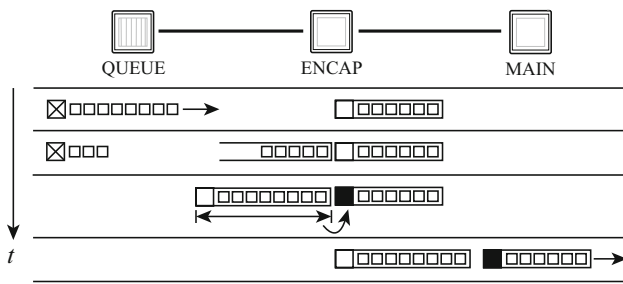


Fig. 4 Inter-process communication in the serviced node

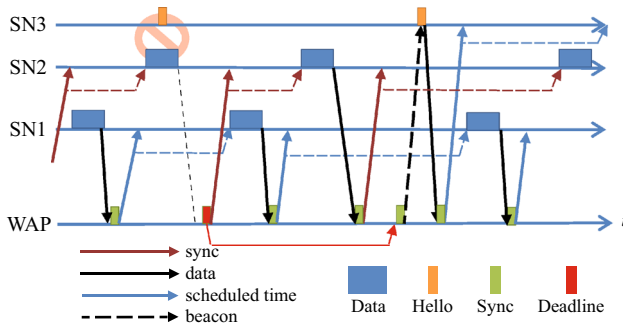


Fig. 5 Frame Exchange between multiple serviced nodes and the wireless access point

work layer packets (typically IP) coming from the queue and encapsulates these into a jumbo frame. Once the frame is built, its size (in bits) is translated into a slot duration time (seconds) using the transmission bit rate (b/s). This is the amount of time requested by the SN to transmit the next frame. The computed time, which is used to synchronize this frame, is inserted into a previously stored frame. Note: It should be mentioned that the size could be stored directly and the WAP can perform the translation to time, both techniques have advantages. The previous frame is sent to the main processor, while the recently encapsulated frame is temporarily stored. Since the recently built frame triggers the transmission of the previously stored frame, this process is referred to as a *push* (i.e. the arriving frame *pushes* the stored one). This continues until the queue is empty or a specified maximum is reached. To better illustrated this process see Fig. 4.

3.2.3 Communication dynamics of VST-TDMA

To stack the frames the following rules are applied, please refer to Fig. 5 to aid the discussion. The task of linking and servicing the first SN is trivial, since there are no other active transmissions. If various nodes are sharing the channel and an inactive node turns active, such that it must enter the sharing cycle, it will send a hello frame. The processes are stacked such that there is insufficient time to transmit in between frames; this will cause collisions. When a collisions occurs,

the WAP sends a new schedule time to the expected SN with the maximum allocation time (assuming the sync field could not be recovered). Since this is the last event a beacon signal is scheduled after this allowing enough time for a hello frame to be retransmitted.

Because there is a scheduled SN the unlinked SN has to wait until the beacon signal to establish a link. Once the WAP has serviced and rescheduled the linked SNs, it sends the beacon signal. The unlinked SN detects that this is a broadcast message (not a hello frame response) and retransmits the hello frame and holds on to the data until the next cycle. The WAP links the SN and from there on frame exchange returns to its routine, but with an additional SN.

3.2.4 Energy self-sustainability support under VST-TDMA

Energy efficiency is an essential feature in any wireless system. Self-sustainability is an attractive quality that frees the nodes from a fixed power supply. To support self-sustainability a node must pose an energy harvesting device and this device must generate energy at a greater rate than the discharge rate of the sleep state. Using VST-TDMA an idle process can be inserted in a cyclic manner to help restore battery loss. The following set of equations describe how to compute the necessary time needed to attain self-sustainability. The self-sustainability condition is given as follows:

$$E^{\otimes} \geq \sum_{i \in State} E_i^{\odot} + E_{sleep}^{\odot} \tag{2}$$

The energy harvested is given by E^{\otimes} and all the discharge states are denoted by the set E_i^{\odot} , except for the energy consumed by the sleep state, which is denoted by E_{sleep}^{\odot} . i denotes the space of states, i.e., transmission, reception, synchronization, etc. (except sleep). Because $E = P t$, (2) can be solved for the sleep time. To find the sleep time expression we assume that the system is continuously harvesting energy (i.e. $t^{\otimes} = \sum_{i \in State} t_i^{\odot} + t_{sleep}^{\odot}$) and that the discharge rate of all the states is greater than the energy harvesting rate, with the exception of the sleep state, then we have the following expression:

$$t_{sleep} \geq \frac{\sum_{i \in State} (P_i^{\odot} - P^{\otimes}) t_i^{\odot}}{P^{\otimes} - P_{sleep}^{\odot}} \tag{3}$$

Note that if the discharge rate of all the energy-consuming states, including the sleep state, where lower than the energy harvesting rate then the sleep time would not be necessary and the expression is reduced to $t_{sleep} = 0$. If the energy consumption of the sleep state where greater than the energy harvesting rate then there is no solution to the inequality (i.e. it is impossible to achieve energy self-sustainability). If

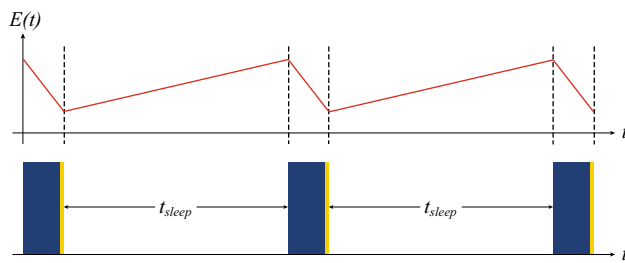


Fig. 6 Energy harvesting effect on the node energy levels as a function of time

the node determines it should enter energy self-sustainability mode, based on predefined criteria, it will measure the amount of energy (or power) it consumes in all the states. It informs the WAP of its energy state and that it has switched to energy self-sustainability mode. Once the WAP is informed it computes the sleep time using (3). The WAP uses this information to schedule the node, inserting an idle time between frames (see Fig. 6). Since the *Sync* frame contains the computed resume time, the node can enter and remain in sleep mode until the synchronization time is reached. This procedure is repeated in every cycle and the sleep time can be adjusted accordingly with the objective of balancing the energy consumed with the energy harvested. This energy self-sustainability mechanism can be applied to various applications such as video streaming, personal health monitoring, playing online video games, synchronizing large amounts of data with the cloud, among many other applications that 5G networks will enable.

4 Discussion and results

This section demonstrates the advantages of using the proposed solutions described in Sect. 3. The simulations include PAPR analysis of SC-FDMA, time savings of VST-TDMA versus legacy TDMA, and charge/throughput trade-off analysis of different sleep-time values, including the self-sustainable and a charge-proportional sleep-time cases.

4.1 PAPR analysis of the proposed system

SC-FDMA has similar throughput performance, and essentially the same overall complexity as OFDMA [7, 10, 16, 38, 39]. A principal advantage of SC-FDMA over OFDM and OFDMA is its lower PAPR. Therefore, in this section we analyze the PAPR of the proposed system using different subcarrier mapping modes and high order modulation schemes. For the different systems implemented, 10^5 uniform random symbol blocks were generated. Applying the criteria in [7, 9], and [8], the PAPR of the pulse shaping filter was measured and analyzed. After calculating the PAPR of each block, the

Table 1 System simulation parameters

Parameter	Value
Technology	SC-FDMA/OFDM
Modulation	QPSK/16QAM
Number of subcarriers	512
Input data block size	64
Spreading factor Q	8
Transmission bandwidth	400 MHz
Block oversampling	4
Subcarrier allocation	Interleaved/localized (only in SC-FDMA)
Uniform random data points	10^5
Roll-off factor	$\alpha = 0.22$
Pulse shaping filter	Root raised cosine (RRC)

data was presented as an empirical complementary cumulative distribution function (CCDF) [40]. The CCDF function measures the probability that a given PAPR exceeds a certain threshold described in our work as $PAPR_0$. Therefore, the CCDF function is given as $(Pr \{PAPR > PAPR_0\})$. Unlike OFDM, the statistical properties of PAPR for single carrier modulations are not easily obtained analytically [7, 9, 39]; therefore, we implemented numerical analysis in our work to examine the PAPR of the proposed system. The total PAPR at the transmitter side is determined by the combination of the technology scheme used and the pulse shaping filter implemented. The PAPR is defined as the ratio of the peak power to the average power of the signal to be transmitted.

Table 1 illustrates the parameters implemented in our simulations, which in general comply with the parameters implemented in [62]. This was done to compare the PAPR performance of the proposed system with OFDM, which has been the technology proposed for the 60 and 70 GHz bands by other researchers [47, 48, 62]. Further, we evaluated the proposed system by using localized and interleaved subcarrier mapping for the SC-FDMA scheme. We implemented high order modulation schemes, such as QPSK and 16QAM, to evaluate PAPR performance in SC-FDMA and OFDM. The 3GPP specifications suggest the use of the RRC pulse at the transmitter side of the BS and UE with a roll-off factor $\alpha = 0.22$ [1, 2]; therefore, we will evaluate the RRC pulse with $\alpha = 0.22$.

In Figs. 7 and 8 we analyze the PAPR performance of the proposed SC-IFDMA, SC-LFDMA, and the traditional OFDM system using QPSK and 16QAM, respectively. It can be seen that the SC-IFDMA system has the lowest PAPR compared to those of the other evaluated systems with a fixed roll-off factor and different modulation schemes. Further, the proposed system completely outperforms the traditional OFDM scheme in terms of PAPR performance. For a proba-

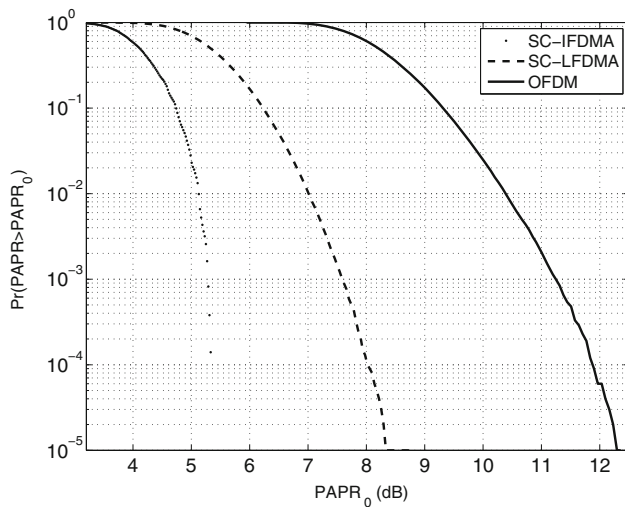


Fig. 7 CCDF of PAPR for the proposed systems and OFDM with $\alpha = 0.22$ and QPSK

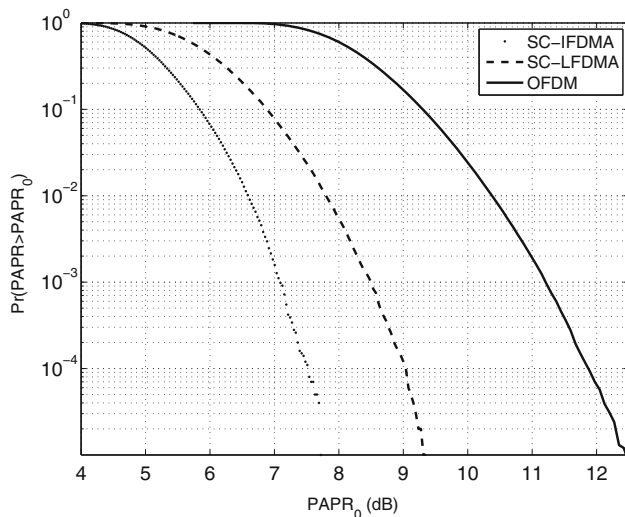


Fig. 8 CCDF of PAPR for the proposed systems and OFDM with $\alpha = 0.22$ and 16QAM

bility of 10^{-4} and using QPSK, the SC-IFDMA system has a $PAPR_0$ of about 5.3 dB, whereas for the OFDM scheme the $PAPR_0$ is about 11.8 dB; therefore, there is a PAPR gain of 6.5 dB for the evaluated system. Similar conclusions are obtained by implementing 16QAM in the evaluated systems.

4.2 Multiplexing access analysis

The time-based multiplexing techniques implemented by VST-TDMA allow it to schedule data efficiently, saving considerable time. To demonstrate the performance capabilities of VST-TDMA it is compared with four MAC protocols: three widely known by the MAC layer community and a recent proposal. The three well-known protocols are Aloha [3], Slotted Aloha [45], and traditional TDMA. Another



Fig. 9 Modeled network topology, four serviced nodes and one wireless access point

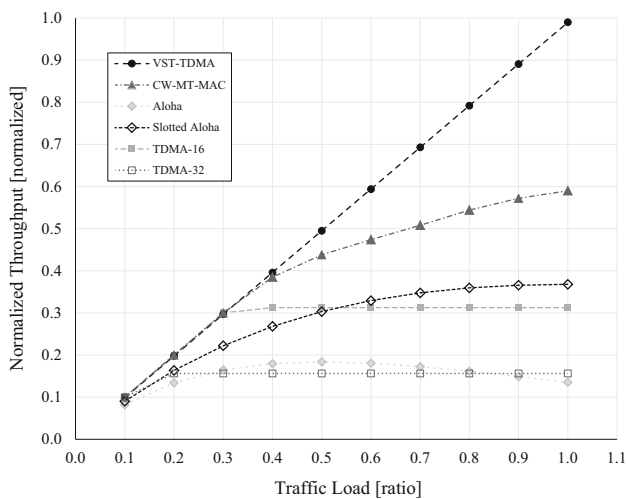
protocol compared is CW-MT-MAC, which is recent work (2014) in 60-GHz WLAN MAC protocols [29], which is an improvement of a previous proposal [30]. CW-MT-MAC has several similarities to VST-TDMA including: the wireless transmission is multiplexed in time, the superframe has a variable length (similar to variable time slot duration, but with less granularity), and it is designed specifically for 60 GHz transmissions. Additionally, even though the throughput is normalized, both work have chosen 1 Gbps as the channel bitrate for the simulations. Among the results obtained by [29], this work uses the best results reported in this publication, which is the CW-MT-MAC case using a wavelength to remote antenna unit (RAU) ratio (λ/R) of 4:5 (80%), that is, for every four available wavelengths there are five RAUs (see Sect. 2.2 or [29] for more information). The network topology consists of one WAP and five SNs as shown in Fig. 9, this is to match nodes per RAU from [29]. A simulation scenario is configured to observe how the protocol handles the traffic with different data transmission loads by observing the resulting throughput. Load here is used in the same context as all nodes start transmitting simultaneously. The link capacity is fixed at 1 Gbps. For VST-TDMA, the load is varied by setting the packets arrival rate at the sender’s queue, this will isolate transport layer effects that can be caused by TCP or UDP packet arrival patterns. The load is evenly distributed among the SNs. The performance of traditional TDMA depends on the amount of slots the cycle has been divided into. Choosing a large number can accommodate many SNs, but the cycle requires more time to serve all nodes (slower maximum throughput). The TDMA’s compared are 16 and 32 slot. Packet sizes in all cases are 1288 bytes. Synchronization frames (only for VST-TDMA) are 20 bytes. The maximum slot time of VST-TDMA is chosen to match the superframe size of CW-MT-MAC. The buffer time (time from the last transmission’s tail to the head of the next) is 160 ns, which is large enough to avoid frame collisions between transmissions in an office environment (48 meters between nodes). The simulation parameters are shown in Table 2 and the results are shown in Fig. 10.

Several observations can be made from Fig. 10. Both traditional TDMA protocols have a peak value for a certain traffic load. In the case for a TDMA with 16 slots (TDMA-16), the maximum throughput that can be achieved, using the common scenario is approximately 31% of the traffic load. For the 32-slot version of TDMA (TDMA-32) the through-

Table 2 MAC protocol simulation parameters

Description	Value
(a) General	
Wireless throughput	1 Gb/s
Packet size	1288 bytes
Max. distance between SN-WAP	48 m
Max. propagation delay	160 ns
Buffer time	160 ns
(b) Additional CW-MT-MAC	
Fiber propagation delay	1 μ s
Available wavelengths	8
RAUs	10
Superframe size ^a	14960 bytes
Scheduling	round-robin algorithm

^a Superframe includes resource requesting frames and data frames for 10 RAUs

**Fig. 10** Normalized throughput performance for different traffic loads

put is reduced further and has a maximum of 16 % of the traffic load. This occurs because for the same size time slot, 32-slot TDMA needs twice the time to cycle through all the slots. If the traffic is been generated by 5 users, only 5 slots will be active. The other slots are reserved for other users. The greater the amount of slots, the more users the WAP can support. Both Aloha and Slotted Aloha are contention-based protocols and exhibit a peak throughput at 0.5 and 1.0 traffic loads, respectively. The reason for observing a peak is because during low traffic loads the channel is under-utilized, but inversely, when the load is too high there is an excessive amount of collisions and the probability of a frame been successfully transmitted decreases with increasing load. In the case of slotted Aloha, i.e., same as Aloha but restricting the start time to the beginning of a slot, the throughput is increased because collisions occur only when you nodes

Table 3 Battery simulation parameters

Description	Value
(a) Setup	
Sleep time	0–1000 ms
Energy harvesting rate	100 μ J/s
Battery energy capacity	25920 J
Battery voltage	3 V
(b) Power	
Operation mode	Power
Sleep	0.09 mW
Transmitting	9.9 mW
Receiving	9.3 mW
Synchronization	6 mW

transmit simultaneously, but there is no longer a chance of a frame colliding with a partially overlapping frame. In the case of CW-MT-MAC, the throughput is constraint by the amount of available wavelengths per RAU. It is a fair assumption that the underlying backbone technology of 60-GHz cells is fiber-optic-based. Since the CW-MT-MAC work reports results for up to 80 % λ/R ratio, an attempt to estimate a ratio of 1:1 (100 %) is done here for a better comparison. The designers of CW-MT-MAC mention that there is a linear relation between throughput and load, with a 92 % efficiency. Results show that adding overhead decreases this to 88–90 %, finally there is an additional 13–15 % drop (25 % total), which is not explained, that causes the 80 % case have less than 60 % throughput. Extrapolating the results of [29] for the λ/R of 1:1, will yields a normalized throughput of 0.75. Finally, VST-TDMA shows a constant efficiency of over 99 %, independent of the traffic load.

4.2.1 Charge aware multiplexing access implementation

VST-TDMA has various advantages. One advantage of VST-TDMA is that it can be programmed to monitor the battery charge and react such that a mobile node does not need to connect to a fixed power supply to charge. The device can estimate the state of charge and dynamically adjust the sleep time to extend the useful remaining charge time. The power-consumption simulation parameters used are drawn from [27] with the exception of the battery energy capacity, as realistic values are in the range of thousands of joules. The parameters used are shown in Table 3. Adding a sleep interval to make up for power loss in a system that has an energy harvesting device present has been suggested in earlier work [21,27]. Having long periods of sleep time will certainly improve the energy efficiency of the system, even make it self-sustainable, but this will cause a throughput trade-off. The throughput reduction is rarely mentioned and when men-

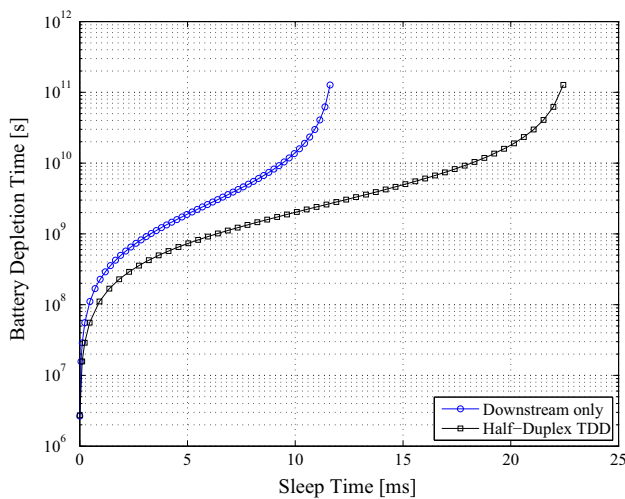


Fig. 11 Sleep time versus battery depletion time for half-duplex TDD and downstream cases

tioned it is mainly to inform the reader of its existence, but there are limited studies of the effects of the sleep interval on the throughput or how to improve the performance of multiplexing techniques that employ the sleep time.

The simulation scenario consist of a WAP and SN pair, where each SN is equipped with an energy harvesting device ($100 \mu\text{J/s}$). The system throughput is 1 Gbps, though the effective throughput can be varied by the insertion of sleep (idle) times. As the sleep time increases the effective throughput will decrease. The effective throughput can be computed as the amount of data transmitted per unit time; for example, if the link capacity is 1 Gbps and the channel is inactive for half of the time then the effective throughput is 500 Mbps. Observing Fig. 11, it can be noticed that the case where the sleep time is zero (no sleep time) the battery will be depleted in under 3×10^6 s, which is approximately one month. This will be the minimum battery depletion time that can occur. When the sleep time is increased to the point the system is self-sustainable, hence called the self-sustainable time, it will yield the maximum necessary time (i.e. any further would be an unnecessary delay) and the system will reach the lowest effective throughput. The asymptotes correspond to the self-sustainable sleep times, i.e., ~ 12 ms for the downstream-only case and ~ 22.5 ms for the TDD (bidirectional) half-duplex case. The half-duplex sleep time is approximately doubled because the sleep time is making up for the power consumed by both upstream and downstream traffic. It is not exactly double because the transmission and reception power consumption parameters are not assumed to be equal. When the sleep time equals the self-sustainable time the battery depletion time is infinite in theory. As we can see from Fig. 11, the last measurable point (when the system is near self-sustainable) occurred once the battery depletion time had exceeded 10^{11} s, or three thousand years, which is

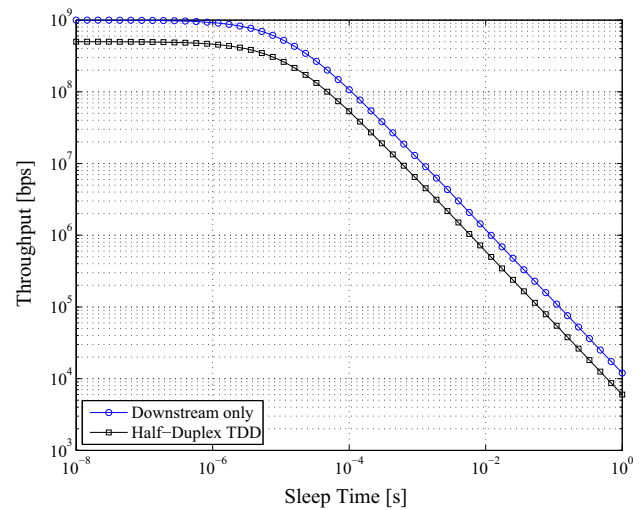


Fig. 12 Throughput dependence on sleep time

clearly overkill. This indicates that the node does not require to operate at such conservative sleep times. Mapping the self-sustainable time to the throughput (see Fig. 12), it can be seen that the throughput for the unidirectional case will be approximately 1 Mbps. For the purpose of comparison lets assume that the life of a sensor was 20 years ($\sim 6.3 \times 10^8$ s). Observing again the downstream-only case this corresponds to a sleep time of 2.5 ms (Fig. 11). This is equivalent to a throughput in the tens of Mbps an order of magnitude improvement over the self-sustainable case. This is assuming the battery is never charged by another source other than the energy harvesting device. If the active/inactive ratio is modified the improvement will vary, so the exact improvement factor will depend on the specific application. A higher active/inactive ratio corresponds to a better throughput performance, but worse energy conservation scheme. Therefore, if the device could detect the user's usage profile it could dynamically adjust the sleep times to maintain an optimal throughput without draining the battery.

Battery health is an important topic and its life can be significantly extended by taking a simple measure. Though the main focus on this work is not centered on the battery degradation, it is suggested in various work [41–43] to keep the level of Lithium-ion batteries above a certain threshold to extend its life. The more frequent the battery is charged the longer the life is extended, i.e., it is better to discharge 10 % of the battery and recharge to full capacity 10 times than to discharge 50 % of the battery and recharge to full capacity 2 times. Nevertheless, it is strongly suggested to not let the battery discharge over 80 % of its total capacity otherwise significant irreversible damage will occur to the battery cells. For this reason the following set of simulations take this suggestion into consideration. To avoid falling below the 20 % of the total available charge threshold the sleep time is adjusted

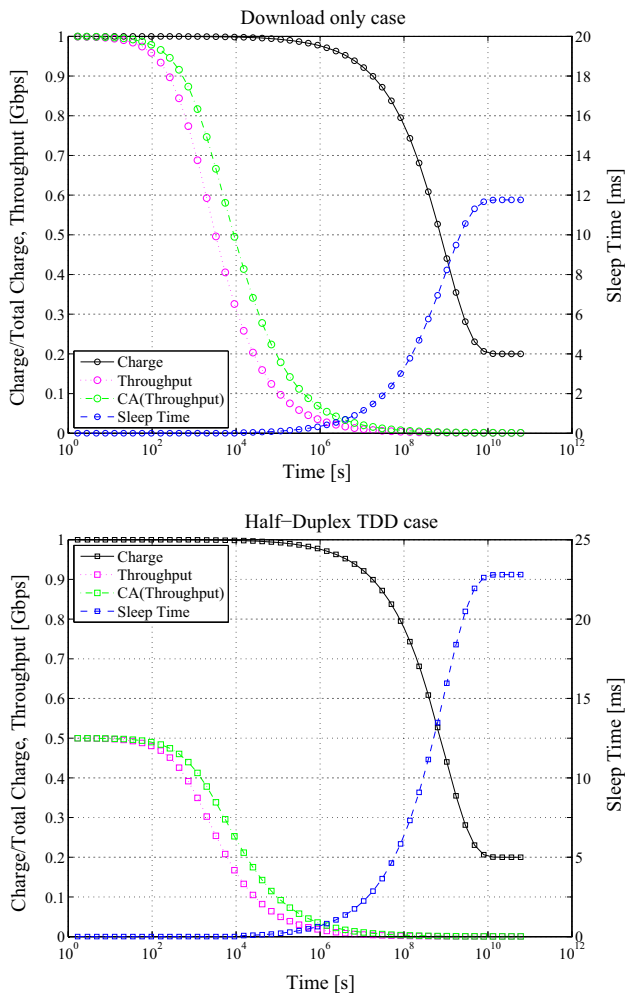


Fig. 13 Charge, sleep time and throughput information for the download only case (top) and the half-duplex TDD case (bottom)

such that it reaches the self-sustainable time when the battery charge reaches 20 % of the total capacity. As a function of the charge state this can be achieved by enforcing the following equality:

$$t_{sleep}(t) = 5/4 \cdot \left(t_{SSS} - t_{SSS} \cdot \frac{charge(t)}{charge_{total}} \right) \quad (4)$$

The following simulations were performed under two cases. A downstream-only case, where the only upstream information is the synchronization, and a half-duplex TDD bidirectional symmetric-link case. An upstream only case would behave in the same manner from a multiplexing standpoint (e.g. sensor network). By implementing the dynamic sleep-time behavior, from (4), the battery will reach 20 % of the total charge in approximately 1×10^{10} s or 300 years (see Fig. 13), which is still very conservative. When this happens the sleep time is equal to the self-sustainable sleep time, which means that the throughput has dropped

approximately three orders of magnitude. By implementing the energy conservation model described by (4), the charge can be preserved for a much longer period than if no sleep is implemented and the throughput is significantly higher than the throughput that results when the system is running at the self-sustainable sleep time. Comparing the no-sleep discharge rate with the energy conservation model discharge rate it can be observed that to reach 20 % of the total charge the no-sleep scheme will drain the charge in $8640 \cdot 3/0.099 = 2.6 \times 10^6$ s, which is 30.3 days or one month. Using the energy conservation scheme in a 30-day interval the battery will only drop 5 % of the total charge. Comparing from a throughput standpoint using the energy conservation scheme after a month of discharging the throughput will drop to ~ 20 Mbps. A more relevant metric than the current throughput is the cumulative average throughput or CA (throughput), as it indicates the overall data rate. The CA(throughput) is defined as the overall throughput perceived up to that point in time (i.e., $CA[throughput]_n = \frac{1}{time_n} \sum_{i=0}^n throughput_i \cdot (time_i - time_{i-1})$, assuming $time_0 = 0$, or alternatively $CA[throughput]_t = \frac{1}{t} \int_0^t throughput(\tau) d\tau$). Continuing to compare the 30-day interval, from Fig. 13 (top) it can be observed that the overall throughput for 2.6×10^6 s corresponds to ~ 50 Mbps. This is a significant improvement as it is only 20 times lower than the no-sleep scheme and 50 times greater than the self-sustainable case. Considering that the charge (as mentioned before) is only 5 % less than the self-sustainable case and nearly 5 times better than the no-sleep case, it is a reasonable trade-off. The half-duplex TDD case is transmitting in both directions, but only the throughput of one direction is analyzed (from the perspective of the end user). Since it is transmitting twice the amount of information it consumes nearly twice the amount of energy (transmitter and receiver energy consumption are slightly different) and therefore the sleep time will nearly double (188 % increase), as shown in Fig. 13 (bottom). This will cause the throughput to decrease to ~ 25 Mbps. It should be stressed that this is a generic case and the aggressiveness or leniency of the model described by (4) can be adjusted to a particular application.

To provide further comparison, five cases are studied and compared from a throughput and charge point of view. These are the no-sleep case (sleep time = 0), the case where the sleep time equals the self-sustainable sleep time (SST) ($t_{sleep} = SST$), the case where sleep time equals SST/10 ($t_{sleep} = SST/10$), the $t_{sleep} = SST/100$ case, and the case described by (4) where the sleep time is proportional to the battery charge, where the relation is $t_{sleep} \propto 1 - \frac{charge}{charge_{total}}$. As seen in Fig. 14, the traces that correspond to the no-sleep-time ($t_{sleep} = 0$) or a fraction of SST, show that the discharge rate for these cases is quicker than the proportional case. No cases outperform the self-sustainable case in terms of energy preservation. From a data rate point of view, as seen on Fig. 15, the throughput for the proportional sleep

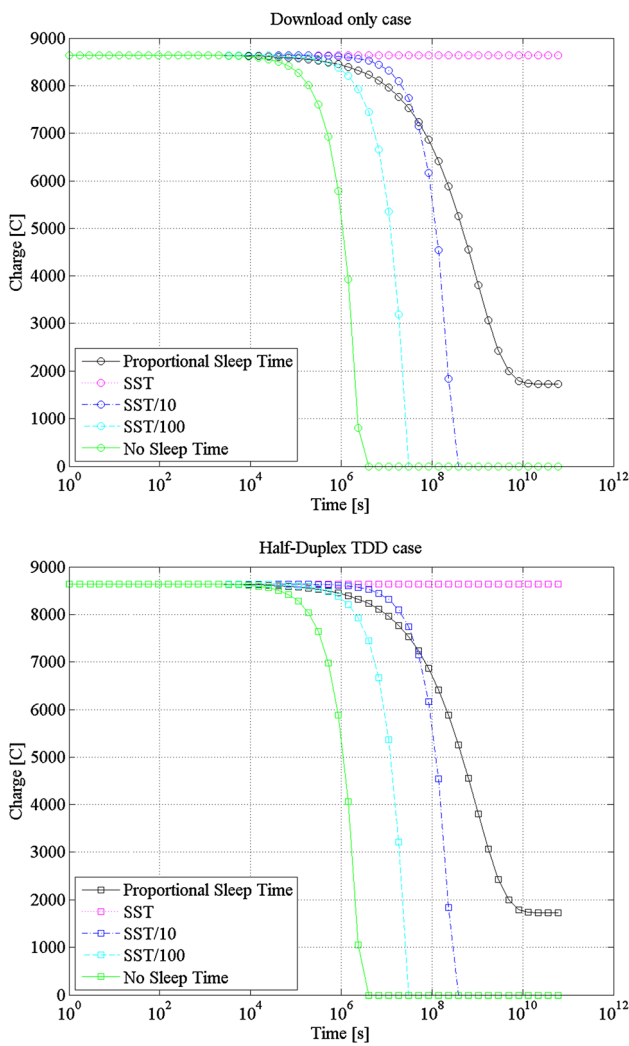


Fig. 14 Charge comparison for the download only case (*top*) and the half-duplex TDD case (*bottom*)

time case is higher for the earlier region, which is generally the most important region. In these plots (for both download only and half-duplex TDD cases) the proportional sleep time case starts at the no-sleep throughput and ends in the self-sustainable sleep-time throughput. This shows that the model behaves as designed. Another interesting point is that the throughput of the dynamic sleep time case will exhibit a throughput greater than the $t_{sleep} = SST/100$ case for $\sim 1 \times 10^5$ s (approximately 27 h) and greater than the $t_{sleep} = SST/10$ case for $\sim 1 \times 10^7$ s (nearly 4 months). This shows that as the battery charge decreases, it is significantly more challenging to maintain a high throughput for a prolonged period of time while attempting to conserve energy. Overall this shows that the measures taken to preserve energy while maintaining a high throughput have a considerable improvement and can be further improved with a specific target application.

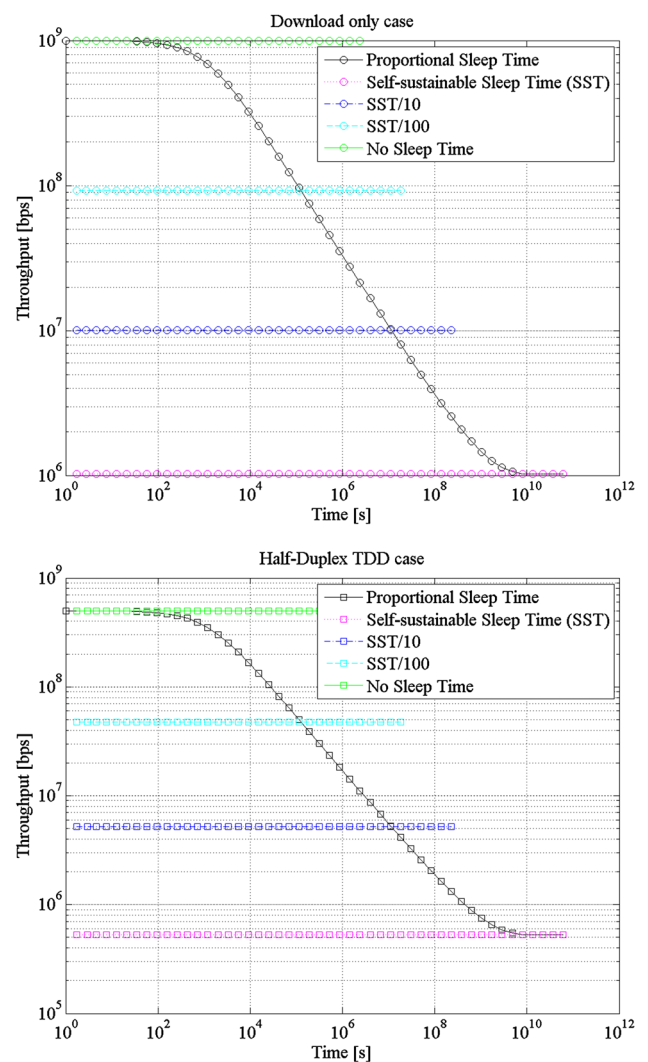


Fig. 15 Throughput comparison for the download only case (*top*) and the half-duplex TDD case (*bottom*)

5 SC-FDMA and VST-TDMA synergy

One of the main benefits of implementing SC-FDMA alongside with VST-TDMA is that the energy savings produced by SC-FDMA will yield higher throughputs using VST-TDMA under the proportional scheme described in section 4.2.1. This means higher independence and greater transmission bit rates for longer duration. Greater energy savings will push the curves shown in Fig. 15 toward the right, which means greater throughput for the same amount of battery use time. And additional advantage of the SC-FDMA/VST-TDMA synergy is that SNs do not require to switch or tune to specific frequencies, they will always use the whole allowable spectrum. This implies that the system can be further simplified, meaning a reduction in cost and computational overhead due to frequency tuning at the software level.

6 Conclusions

A set of bottom-layer solutions is proposed for 60 GHz millimeter-wave systems. The solutions include a multiplexing access protocol with an energy-aware technique that is embedded in the access protocol, and SC-FDMA is proposed as the technology to be implemented at the physical layer. Each attribute is discussed independently and its benefits are described below.

SC-FDMA was proposed as the technology to be implemented at the physical layer to comply with the initial version of the IEEE 802.16-2001 standard, and because SC-FDMA is characterized by having a lower PAPR compared to multi-carrier systems. The proposed system was evaluated in terms of PAPR by using the RRC pulse shaping filter and $\alpha = 0.22$ to comply with the parameters indicated by the 3GPP standard. Through simulations it was shown that the proposed system outperformed the OFDM system in terms of PAPR.

The multiplexing access protocol called VST-TDMA is a time-based multiplexing technique. VST-TDMA is very versatile, as it can reserve time for processes other than multiplexing data, the ability to dynamically adjust the energy consumption, and the capability to shift the bandwidth to where it is needed (upstream/downstream/symmetric). This protocol takes advantage of the reduced cell size under the assumption that the number of users is significantly reduced. Considering that not all users are occupying the cell's base station at the same time, the available bandwidth is better utilized by a time multiplexing access technique rather than multiplexing in the frequency domain, where unused bands are wasted, or using CSMA, where neighbor discovery is unreliable. VST-TDMA showed a significant increase in traffic flow efficiency (i.e. increase in the overall throughput) where the throughput to traffic load ratio (efficiency) was consistently over 99 % for the traffic load range of 0.0–1.0 range. This is an improvement over other recent MAC protocol proposals, such as [29].

Another important characteristic of VST-TDMA is its capability to find a self-sustainable state under the presence of an energy harvesting device. Results prove that by balancing the charging time with the discharging time, self-sustainability is feasible under the condition that the power consumed by the sleep state is lower than the energy harvesting rate. The energy self-sustainability is achieved at the cost of lowering the throughput. Slowing the transmission rate allows for the system to reduce energy consumption, if the usage is slowed enough a balance can be found (i.e., the energy harvester can compensate the energy loss). The self-sustainable sleep time for a downstream-only case is ~ 12 ms (from Fig. 11), which corresponds to a throughput of ~ 1 Mbps (from Fig. 12), a throughput significantly lower than the channel capacity. Typical values for energy consumption yield that a system capable of transmitting at

1 Gbps would be slowed down to just a few Mbps. Though, if the device could detect the user's usage profile it could force lower sleep times to maintain the throughput higher with the a-priori knowledge of the inactive intervals that allow the device to recharge. Therefore the perceived throughput will be much greater with the same energy harvesting capability. The reduced throughput experience under self-sustainability can be relieved by implementing a dynamic sleep time that is proportional to the available charge. For the particular case 30-day case discussed in this work, the overall throughput was increased to 50 Mbps (50 times better than the self-sustainable case) with a charge drop of 5 %.

Acknowledgments This work is partially funded by project FONDECYT No. 11121655, Fondo Nacional de Desarrollo Científico y Tecnológico and Grant U-INICIA 11/14, Vicerrectoría de Investigación y Desarrollo (2011), Universidad de Chile. This work is partially funded by the Program U-INICIA VID 2014, Grant No. UI-02/2014, Universidad de Chile.

Open Access This article is distributed under the terms of the Creative Commons Attribution License which permits any use, distribution, and reproduction in any medium, provided the original author(s) and the source are credited.

References

1. 3rd Generation Partnership Project (3GPP): Universal mobile telecommunications system (UMTS); base station BS radio transmission and reception FDD. Tech. Rep. 125.104, European Telecommunications Standards Institute (20014).
2. 3rd Generation Partnership Project (3GPP): Universal mobile telecommunications system (UMTS); user equipment UE radio transmission and reception FDD. Tech. Rep. 125.101, European Telecommunications Standards Institute (2014).
3. Abramson, N. (1970). The aloha system: another alternative for computer communications. In: Proceedings of the November 17–19, 1970, fall joint computer conference, pp. 281–285. ACM
4. Amitay, N. (1992). Resource auction multiple access (rama): efficient method for fast resource assignment in decentralised wireless pcs. *Electronics Letters*, 28(8), 799–801.
5. Andersin, M., Mandayam, N. B., & Yates, R. D. (1998). Subspace based estimation of the signal to interference ratio for TDMA cellular systems. *Wireless Networks*, 4(3), 241–247.
6. Atmaca, S., Karahan, A., Ceken, C., & Erturk, I. (2014). A new MAC protocol for broadband wireless communications and its performance evaluation. *Telecommunication Systems*, 57(1), 13–23. Springer.
7. Azurdia-Meza, C., Lee, K. J., & Lee, K. S. (2012). PAPR reduction in SC-FDMA by pulse shaping using parametric linear combination pulses. *IEEE Communications Letters*, 16(12), 2008–2011.
8. Azurdia-Meza, C. A., Lee, K. J., & Lee, K. S. (2012). PAPR reduction by pulse shaping using Nyquist linear combination pulses. *IEICE Electronics Express*, 9(19), 1534–1541.
9. Azurdia-Meza, C. A., Lee, K. J., & Lee, K. S. (2013). PAPR reduction in single carrier FDMA uplink by pulse shaping using a $\beta - \alpha$ filter. *Wireless Personal Communications*, 71(1), 23–44.
10. Berardinelli, G., de Maestro Ruiz de Temino, L. A., Frattasi, S., Rahman, M. I., & Mogensen, P. (2008). OFDMA vs. SC-FDMA: Performance comparison in local area IMT-A scenarios. *IEEE Wireless Communications*, 15(5), 64–72.

11. Boccardi, F., Health, R. Jr, Lozano, A., Marzetta, T. L., & Popovski, P. (2014). Five disruptive technology directions for 5G. *IEEE Communications Magazine*, 52(2), 74–80.
12. Chen, S., & Zhao, J. (2014). The requirements, challenges, and technologies for 5G of terrestrial mobile telecommunication. *IEEE Communications Magazine*, 52(5), 5.
13. Chen, X., Azim, A., Liu, X., Fischmeister, S., & Ma, J. (2014). DTS: Dynamic TDMA scheduling for networked control systems. *Journal of Systems Architecture*, 60(2), 194–205.
14. Chien, H. C., Hsueh, Y. T., Chowdhury, A., Yu, J., & Chang, G. K. (2010). Optical millimeter-wave generation and transmission without carrier suppression for single- and multi-band wireless over fiber applications. *Journal of Lightwave Technology*, 28(16), 2230–2237.
15. Choi, J., Kang, D., Kim, D., Park, J., Jin, B., & Kim, B. (2009). Power amplifiers and transmitters for next generation mobile handset. *Journal of Semiconductor Science and Technology*, 9(4), 249–256.
16. Ciocchina, C., & Sari, H. (2010). A review of OFDMA and single-carrier FDMA and some recent results. *Advances in Electronics and Telecommunications*, 1(1), 35–40.
17. Daniels, R. C., Murdock, J. N., Rappaport, T. S., & Heath, R. W. Jr. (2010). 60 GHz wireless: Up close and personal. *IEEE Microwave Magazine*, 11(7), 44–50.
18. De Rango, F., Perrotta, A., Marano, S. (2007). Qos-croma: An on-demand time-slotted mac protocol with qos support for wireless ad hoc networks. In: IEEE 4th International Symposium on Wireless Communication Systems, 2007. ISWCS 2007, pp. 706–710.
19. Eklund, C., Marks, R., & Stanwood, K. (2002). IEEE standard 802.11: A technical overview of the wirelessMAN air interference for broadband wireless access. *IEEE Communications Magazine*, 40(6), 90–107.
20. Estevez, C., Kailas, A. (2012). Energy-efficient process-stacking multiplexing access for 60-ghz mm-wave wireless personal area networks. In: IEEE Annual International Conference of the Engineering in Medicine and Biology Society (EMBC), 2012, pp. 2084–2087.
21. Estevez, C.I., Wei, J., Kailas, A., Fuentealba, D., Chang, G.K. (2011). Very-high-throughput millimeter-wave system oriented for health monitoring applications. In: 13th IEEE International Conference on e-Health Networking Applications and Services (Healthcom), 2011, pp. 229–232. IEEE
22. Hammoudeh, A. M., & Allen, G. (1995). Millimetric wavelengths radiowave propagation for line-of-sight indoor microcellular mobile communications. *IEEE Transactions on Vehicular Technology*, 44(3), 449–460.
23. Huang, G., Nix, A., Armour, S. (2007). Impact of radio resource allocation and pulse shaping on papr of SC-FDMA signals. In: IEEE 18th International Symposium on Personal, Indoor and Mobile Radio Communications, 2007. PIMRC 2007. pp. 1–5. IEEE
24. IEEE 802.16-2001: IEEE standard for local and metropolitan area networks part 16: air interface for fixed broadband wireless access systems. Tech. rep., IEEE (2002).
25. IEEE 802.16-2012: Revision of IEEE std 802.16. Tech. rep., IEEE (2012).
26. ECMA International. (2010). *Standard ECMA-387: High rate 60 GHz PHY, MAC and HDMI PALs*. Geneva: ECMA International.
27. Jian, W., Chowdhury, A., Jia, Z., Estevez, C. I., & Chang, G. K. (2010). Energy-efficient multi-access technologies for very-high-throughput avionic millimeter wave, wireless sensor communication networks. *Journal of Lightwave Technology*, 28(16), 2398–2405.
28. Jian, W., Estevez, C., Chowdhury, A., Jia, Z., Wang, J., Yu, J., Chang, G.K. (2010). A hybrid MAC protocol design for energy-efficient very-high-throughput millimeter wave, wireless sensor communication networks. In: Asia Communications and Photonics Conference and Exhibition, pp. 79,890Q–79,890Q. (International Society for Optics and Photonics)
29. Kalfas, G., Maniotis, P., Markou, S., Tsiokos, D., Pleros, N., Alonso, L., et al. (2014). Client-weighted medium-transparent MAC protocol for user-centric fairness in 60 GHz radio-over-fiber w lans. *Journal of Optical Communications and Networking*, 6(1), 33–44.
30. Kalfas, G., & Pleros, N. (2010). An agile and medium-transparent MAC protocol for 60 GHz radio-over-fiber local access networks. *Journal of Lightwave Technology*, 28(16), 2315–2326.
31. Kano, H., Yoshizawa, S., Gunji, T., Saito, T., Miyana, Y. (2010). Development of 600 Mbps 2 × 2 mimo-ofdm baseband and rf transceiver at 5 GHz band. In: IEEE International Symposium on Communications and Information Technologies (ISCIT), 2010. pp. 891–894.
32. Kim, J.G., Widjaja, I. (1996). Prma/da: A new media access control protocol for wireless atm. In: IEEE International Conference on Communications, 1996. ICC'96, Conference Record, Converging Technologies for Tomorrow's Applications, 1996. vol. 1, pp. 240–244. IEEE
33. Koonen, A., & Larrodé, M. G. (2008). Radio-over-MMF techniquespart II: Microwave to millimeter-wave systems. *Journal of Lightwave Technology*, 26(15), 2396–2408.
34. Kouroshnezhad, S., Zokaei, S., Yeganeh, H., Sayad Haghighi, M. (2008). Slot reservation demand assignment multiple access control protocol for signalling of telephony traffic via geo satellite. In: 10th International Conference on Advanced Communication Technology, 2008. ICACT 2008. vol. 1, pp. 693–698. IEEE
35. Lan, Z., Sum, C. S., Wang, J., Baykas, T., Kojima, F., Nakase, H., et al. (2009). Relay with deflection routing for effective throughput improvement in Gbps millimeter-wave WPAN systems. *IEEE Journal on Selected Areas in Communications*, 27(8), 1453–1465.
36. Mohamed, N., Idrus, S., Mohammad, A. (2008). Review on system architectures for the millimeter-wave generation techniques for rof communication link. In: IEEE International RF and Microwave Conference, 2008. RFM 2008. pp. 326–330.
37. Myung, H. G., & Goodman, D. J. (2008). *Introduction to single carrier FDMA*. New York: Wiley.
38. Myung, H.G., Lim, J., Goodman, D.J. (2006). Peak-to-average power ratio of single carrier FDMA signals with pulse shaping. In: IEEE 17th International Symposium on Personal, Indoor and Mobile Radio Communications, 2006. pp. 1–5. IEEE
39. Myung, H. G., Lim, J., & Goodman, D. J. (2006). Single carrier FDMA for uplink wireless transmission. *IEEE Vehicular Technology Magazine*, 1(3), 30–38.
40. Nee, Rv, & Prasad, R. (2000). *OFDM for wireless multimedia communications*. Norwood: Artech House, Inc.
41. Olivares, B. E., Muñoz, C., Orchard, M. E., & Silva, J. F. (2013). Particle-filtering-based prognosis framework for energy storage devices with a statistical characterization of state-of-health regeneration phenomena. *IEEE Transactions on Instrumentation and Measurement*, 62(2), 364–376.
42. Orchard, M., Hevia-Koch, P., Zhang, B., & Tang, L. (2013). Risk measures for particle-filtering-based state-of-charge prognosis in lithium-ion batteries. *IEEE Transactions on Industrial Electronics*, 60(11), 5260–5269.
43. Orchard, M. E., Cerda, M. A., Olivares, B. E., & Silva, J. F. (2012). Sequential monte carlo methods for discharge time prognosis in lithium-ion batteries. *International Journal of Prognostics and Health Management*, 3(2), 1–12.
44. Rappaport, T. S., Sun, S., Mayzus, R., Zhao, H., Azar, Y., Wang, G. N., et al. (2013). Millimeter wave mobile communications for 5G cellular: It will work!. *IEEE Access*, 1, 335–349.

45. Roberts, L. G. (1975). Aloha packet system with and without slots and capture. *ACM SIGCOMM Computer Communication Review*, 5(2), 28–42.
46. Roh, W., Seol, J. Y., Park, J. H., Lee, B. H., Lee, J. K., Lee, J. S., et al. (2014). Millimeter-wave beamforming as an enabling technology for 5G cellular communications: theoretical feasibility and prototype results. *IEEE Communications Magazine*, 52(2), 106–113.
47. Shao, Y., Wang, Y., & Chi, N. (2013). 60-GHz RoF system with low PAPR 16QAM-OFDM downlink using PTS segmentation. *Photonics Technology Letters, IEEE*, 25(9), 855–858. IEEE Photonics Society.
48. Shoji, Y., Choi, C. S., & Ogawa, H. (2006). 70-GHz-band OFDM transceivers based on self-heterodyne scheme for millimeter-wave wireless personal area network. *IEEE Transactions on Microwave Theory and Techniques*, 54(10), 3664–3674.
49. Siamarou, A. G., & Al-Nuaimi, M. (2010). A wideband frequency-domain channel-sounding system and delay-spread measurements at the license-free 57-to 64-GHz band. *IEEE Transactions on Instrumentation and Measurement*, 59(3), 519–526.
50. Singh, S., Ziliotto, F., Madhow, U., Belding, E.M., Rodwell, M.J. (2007). Millimeter wave WPAN: cross-layer modeling and multi-hop architecture. In: 26th IEEE International Conference on Computer Communications INFOCOM 2007. pp. 2336–2340.
51. Sthapit, P., & Pyun, J. Y. (2013). Medium reservation based sensor MAC protocol for low latency and high energy efficiency. *Telecommunication Systems*, 52(4), 2387–2395.
52. Su, H., & Zhang, X. (2009). Battery-dynamics driven tdma MAC protocols for wireless body-area monitoring networks in healthcare applications. *IEEE Journal on Selected Areas in Communications*, 27(4), 424–434.
53. Sum, C. S., Funada, R., Wang, J., Baykas, T., Rahman, M. A., & Harada, H. (2009). Error performance and throughput evaluation of a multi-gbps millimeter-wave WPAN system in the presence of adjacent and co-channel interference. *IEEE Journal on Selected Areas in Communications*, 27(8), 1433–1442.
54. Sum, C. S., Lan, Z., Funada, R., Wang, J., Baykas, T., Rahman, M., et al. (2009). Virtual time-slot allocation scheme for throughput enhancement in a millimeter-wave multi-Gbps WPAN system. *IEEE Journal on Selected Areas in Communications*, 27(8), 1379–1389.
55. Van Dam, T., Langendoen, K. (2003). An adaptive energy-efficient MAC protocol for wireless sensor networks. In: Proceedings of the 1st international conference on Embedded networked sensor systems, pp. 171–180. ACM
56. Viterbi, A. (1991). Wireless digital communication: A view based on three lessons learned. *IEEE Communications Magazine* p. 33
57. Walke, B. H., Mangold, S., & Berlemann, L. (2007). *IEEE 802 wireless systems: protocols, multi-hop mesh/relaying, performance and spectrum coexistence*. New York: Wiley.
58. Wang, C. X., Haider, F., Gao, X., You, X. H., Yang, Y., Yuan, D., et al. (2014). Cellular architecture and key technologies for 5G wireless communication networks. *IEEE Communications Magazine*, 52(2), 122–130.
59. Wang, J., Lan, Z., Pyo, C. W., Baykas, T., Sum, C. S., Rahman, M. A., et al. (2009). Beam codebook based beamforming protocol for multi-gbps millimeter-wave WPAN systems. *IEEE Journal on Selected Areas in Communications*, 27(8), 1390–1399.
60. Wei, H.Y., Ganguly, S., Izmailov, R., Haas, Z.J. (2005). Interference-aware IEEE 802.16 wimax mesh networks. In: Vehicular Technology Conference, 2005. VTC 2005-Spring. 2005 IEEE 61st, vol. 5, pp. 3102–3106.
61. WG802.11 - Wireless LAN Working Group: IEEE standard for information technology telecommunications and information exchange between systems local and metropolitan area networks specific requirements part 11: Wireless lan medium access control (mac) and physical layer (phy) specifications amendment 3: Enhancements for very high throughput in the 60 GHz band. Tech. rep., IEEE (2012).
62. Winkler, F., Fischer, E., Grass, E., Fischer, G. (2005). A 60 GHz OFDM indoor localization system based on DTDOA. In: 14th Information Society Technologies Mobile and Wireless Communications Summit. Dresden, Germany
63. Ye, W., Heidemann, J., & Estrin, D. (2004). Medium access control with coordinated adaptive sleeping for wireless sensor networks. *IEEE/ACM Transactions on Networking*, 12(3), 493–506.
64. Yu, Q., Zhou, H. (2006). Advanced mac protocol with adjustable sleep mode for wireless sensor networks. In: International Conference on Wireless Communications, Networking and Mobile Computing, 2006. WiCOM 2006. pp. 1–4.
65. Zheng, T., Radhakrishnan, S., Sarangan, V. (2005). Pmac: an adaptive energy-efficient mac protocol for wireless sensor networks. In: Proceedings of the 19th IEEE International Parallel and Distributed Processing Symposium, 2005. pp. 8-pp.



Claudio Estevez received his B.S. degree in electrical and computer engineering from the University of Puerto Rico, Mayaguez, PR, USA, 2001; his M.S. degree in electrical and computer engineering with a minor in optical engineering from the University of Alabama in Huntsville, Huntsville, AL, USA, 2003; and his Ph.D. degree in electrical and computer engineering and with a minor in computer science from the Georgia Institute of Technology, Atlanta, GA, USA, 2010. In 2011, he was hired as an assistant professor by the electrical engineering department at Universidad de Chile. In 2012, he obtained a [Chilean] national research grant (FONDECYT) to study MAC protocols in WPAN using 60 GHz. In the same year he was appointed coordinator of the Communication Networks M.Eng. Program. In 2013, he obtained a [Chilean] national research grant (FONDEF) to study remote polysomnographic monitoring. His research interests include: Connection-oriented transport protocols, network fairness study, MAC-layer protocols in WPAN, 60-GHz WPAN applications, cloud computing with data mining/warehousing, wireless body area networks, remote healthcare.



Cesar Azurdia received the B.Sc. degree in electrical engineering from Universidad del Valle de Guatemala, Guatemala in 2005, and the M.Sc. degree in electrical engineering from Linnaeus University, Sweden in 2009. In 2013 he obtained the Ph.D degree in Electronics and Radio Engineering, Kyung Hee University, Republic of Korea. He joined the Department of Electrical Engineering, University of Chile as an Assistant Professor in August 2013. He has

served as Technical Program Committee (TPC) member for multiple conferences, as well as a reviewer in journals such as IEEE Communications Letter, IEEE Transactions on Wireless Communications, Wireless Personal Communications, and EURASIP Journal on Advances in Signal Processing. Dr. Azurdia is an IEEE Communications Society

Member. His research interests include topics such as Nyquist's ISI criterion, OFDM-based systems, SC-FDMA, visible light communication systems, 5G & beyond enabling technologies, and signal processing techniques for communication systems.